

## Multiples Waveform Inversion

Dongliang Zhang\*, Wei Dai and Gerard T. Schuster, King Abdullah University of Science and Technology

### SUMMARY

To increase the illumination of the subsurface and to eliminate the dependency of FWI on the source wavelet, we propose multiples waveform inversion (MWI) that transforms each hydrophone into a virtual point source with a time history equal to that of the recorded data. These virtual sources are used to numerically generate downgoing wavefields that are correlated with the backprojected surface-related multiples to give the migration image. Since the recorded data are treated as the virtual sources, knowledge of the source wavelet is not required, and the subsurface illumination is greatly enhanced because the entire free surface acts as an extended source compared to the radiation pattern of a traditional point source. Numerical tests on the Marmousi2 model show that the convergence rate and the spatial resolution of MWI is, respectively, faster and more accurate than FWI.

### INTRODUCTION

An accurate velocity model is the fundamental prerequisite for a high quality migration image. Until recently, such models were estimated by either migration velocity analysis (MVA) (Symes and Kern, 1994) or traveltimes tomography (Langan et al., 1984). These methods, however, only estimate velocity models with intermediate resolution compared to our demand for the highest resolution possible, particularly in imaging below complex geological features such as salt. To reconstruct the higher wavenumbers full waveform inversion (FWI) (Tarantola, 1984; Pratt, 1999) uses both the phase and amplitudes to invert for a highly accurate velocity model. However, it is still a challenge to accurately and reliably invert for velocities beneath salt and complex targets below 5 km or so. Therefore, it is important to discover a means to provide greater seismic illumination below the salt that can enhance the estimation of subsalt velocities.

We propose multiples waveform inversion (MWI) method to invert the velocity. This follows the work of Liu et al. (2011) who migrated surface-related multiples to increase the illumination below salt. The extended source for MWI is created by treating each hydrophone as a virtual point source on the free surface, where the source wavelets are the upgoing reflections recorded by the hydrophones. This natural source of extended energy is numerically propagated as the source field and zero-lag correlated with the backpropagated multiples (recorded at the same hydrophones) to give the misfit gradient (or migration image). The 1st-order and higher-order reflections are extracted from the data by a surface-related multiple elimination method and have the potential to provide much more natural energy below the salt than a localized point source. Hence, the resulting subsalt reflections should have a higher SNR and subsurface coverage than those created by a single point source, and so enhance the capability of subsalt FWI. An added advantage

of this method is that, unlike conventional FWI, knowledge of the source wavelet is not required because the recorded data are used for the source wavelet of the downgoing field.

### METHOD

The MWI algorithm is similar to that of FWI. The misfit function is  $\varepsilon = \frac{1}{2} \sum_{\omega} \sum_g \sum_s |\Delta M(\omega, \mathbf{x}_g, \mathbf{x}_s)|^2$ , where the data residual  $\Delta M(\omega, \mathbf{x}_g, \mathbf{x}_s)$  is defined as  $\Delta M(\omega, \mathbf{x}_g, \mathbf{x}_s) = M(\omega, \mathbf{x}_g, \mathbf{x}_s)_{cal} - M(\omega, \mathbf{x}_g, \mathbf{x}_s)_{obs}$ ,  $M(\omega, \mathbf{x}_g, \mathbf{x}_s)_{cal}$  represents the predicted multiples related to the free surface,  $M(\omega, \mathbf{x}_g, \mathbf{x}_s)_{obs}$  is the observed data. The misfit gradient  $\gamma(\mathbf{x})$  is defined as:

$$\gamma(\mathbf{x}) = \frac{\delta \varepsilon}{\delta s(\mathbf{x})} = \sum_{\omega} \sum_g \sum_s \text{Real}[2\omega^2 s(\mathbf{x}) G(\mathbf{x}|\mathbf{x}_g) \Delta M(\omega, \mathbf{x}_g, \mathbf{x}_s)^* \int G(\mathbf{x}|\mathbf{x}'_g) d(\omega, \mathbf{x}'_g, \mathbf{x}_s) d\mathbf{x}'_g], \quad (1)$$

where,  $\delta \varepsilon$  is the misfit perturbation,  $\delta s(\mathbf{x})$  is the slowness perturbation,  $G(\mathbf{x}'|\mathbf{x}'_g)$  is the Green's function for a source at  $\mathbf{x}'_g$  and an observer at  $\mathbf{x}'$  in the background velocity model, and  $d(\omega, \mathbf{x}'_g, \mathbf{x}_s)$  is the recorded trace that serves as the time history of the virtual source at  $\mathbf{x}'_g$  that includes primary and multiples. The slowness can be iteratively updated by the steepest descent method, until the data residual falls below a specified limit.

### Generation of predicted multiples

The predicted MWI data are the surface-related multiples, so their accurate calculation is crucial for the success of this method. Therefore, the first step is to forward model an extended line of virtual point sources at  $\mathbf{x}_g$ , each having the recorded data  $d(\omega, \mathbf{x}_g, \mathbf{x}_s)$  as the time history for the same shot at  $\mathbf{x}_s$ . In this case, the extended virtual sources yield the wavefield  $P(\omega, \mathbf{x}_g, \mathbf{x}_s)$  in the frequency domain as:

$$P(\omega, \mathbf{x}_g, \mathbf{x}_s) = \int G(\mathbf{x}_g|\mathbf{x}'_g) d(\omega, \mathbf{x}'_g, \mathbf{x}_s) d\mathbf{x}'_g. \quad (2)$$

Here,  $G(\mathbf{x}_g|\mathbf{x}'_g)$  is the harmonic Green's function for a source at  $\mathbf{x}'_g$  and an observer at  $\mathbf{x}_g$ , and  $d(\omega, \mathbf{x}_g, \mathbf{x}_s)$  is the input trace that acts as the time history of the virtual point source. We decompose the Green's function into a sum of two terms:

$$G(\mathbf{x}_g|\mathbf{x}'_g) = G_0(\mathbf{x}_g|\mathbf{x}'_g) + G_1(\mathbf{x}_g|\mathbf{x}'_g), \quad (3)$$

where,  $G_0(\mathbf{x}_g|\mathbf{x}'_g)$  represents the Green's function of the direct wave in a homogeneous medium filled with water, and  $G_1(\mathbf{x}_g|\mathbf{x}'_g)$  represents the Green's function associated with the reflections wavefield in a half-space of water underlain by sediments. We will assume that  $d(\omega, \mathbf{x}_g, \mathbf{x}_s)$  only contains the downgoing reflections from the free surface. Substituting equation 3 into equation 2 yields the new expression:

$$P(\omega, \mathbf{x}_g, \mathbf{x}_s) = \overbrace{\int G_0(\mathbf{x}_g|\mathbf{x}'_g) d(\omega, \mathbf{x}'_g, \mathbf{x}_s) d\mathbf{x}'_g}^{\text{downgoing primary and multiples in water layer}} +$$

## Multiples Waveform Inversion

upcoming multiples in heterogeneous model

$$\int G_1(\mathbf{x}_g|\mathbf{x}'_g)d(\omega, \mathbf{x}'_g, \mathbf{x}_s)d\mathbf{x}'_g \quad (4)$$

Because the extended virtual sources have time histories corresponding to the ongoing primary and multiple reflections recorded at the surface, the first term in equation 4 generates ongoing primary and multiple reflections in a homogeneous water layer, and the second term only contains the ongoing multiple reflections from the heterogeneous background model. In order to compute the ongoing primary and multiples in the 1st term of equation 4, we solve the acoustic wave equation for a homogeneous model with water velocity  $v_0$  to get the pressure field  $P_0(\omega, \mathbf{x}_g, \mathbf{x}_s)$ , which is the first part in equation 4. Subtracting  $P_0(\omega, \mathbf{x}_g, \mathbf{x}_s)$  from equation 4, the predicted  $M(\omega, \mathbf{x}_g, \mathbf{x}_s)$  can be obtained as:

$$\begin{aligned} M(\omega, \mathbf{x}_g, \mathbf{x}_s) &= P(\omega, \mathbf{x}_g, \mathbf{x}_s) - P_0(\omega, \mathbf{x}_g, \mathbf{x}_s) \\ &= \int G_1(\mathbf{x}_g|\mathbf{x}'_g)d(\omega, \mathbf{x}'_g, \mathbf{x}_s)d\mathbf{x}'_g. \end{aligned} \quad (5)$$

### NUMERICAL EXAMPLE

In this section, MWI will be tested on synthetic data calculated for the Marmousi2 model shown in Figure 1a. Here, the predicted data for standard FWI are generated with free-surface boundary conditions and the predicted data for MWI is generated with absorbing boundary conditions that replace the free surface boundary condition. Figure 1b shows the initial velocity model after smoothing the true velocity model. Application of FWI and MWI to these synthetic data results in the FWI and MWI tomograms in Figures 1c and 1d, respectively. The circled areas show that the MWI tomogram is more accurate than the FWI tomogram. Figures 2a and 2b show the data and model residuals for both the MWI and FWI methods and suggest that MWI enjoys a faster reduction in the residual than FWI, and also provides a more accurate velocity model for the same number of iterations. For MWI, the reconstructed earth model must explain a more complex wavefield from an extended source compared to that from a localized point source. This means that there are a fewer number of models that are consistent with the complex data compared to the simpler point source data. This is similar to traveltome tomography where the data consist of simple traveltome picks at each trace, so many smooth models can easily explain the same simple data.

An advantage of MWI compared to FWI is that multiples from an extended source illuminate a much greater region in the subsurface compared to primaries associated with a localized source. This is illustrated in Figure 3ab where the misfit gradient from a CSG is compared to that from an extended source on the surface. If the streamer length increases, the extent of the MWI illumination zone will be even wider compared to the FWI zone, as illustrated in Figure 3cd.

### CONCLUSIONS

We propose multiples waveform inversion to invert the surface-related multiples for the subsurface velocity distribution. In

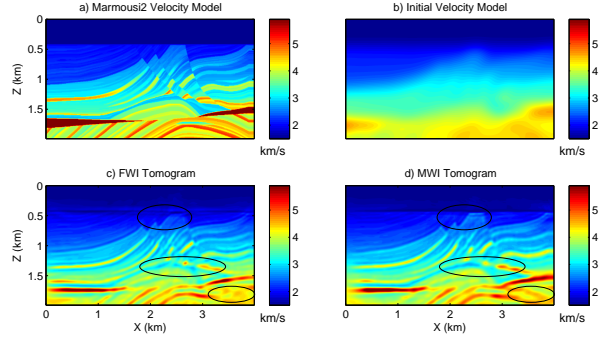


Figure 1: a) Marmousi2 velocity model. b) Initial velocity model. c) FWI and d) MWI tomograms after 100 iterations.

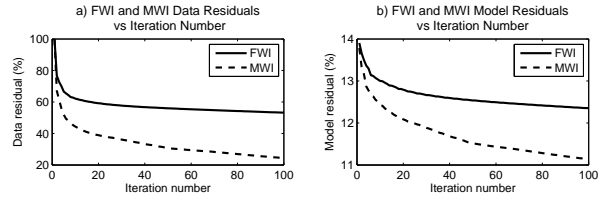


Figure 2: a) Data and b) model residuals for FWI and MWI.

this method, recorded traces are used as the time histories of the virtual sources at the hydrophones and surface-related multiples are the observed data. Compared to standard FWI, the advantages of MWI are that no knowledge of the actual source wavelet is needed, and it enjoys faster convergence and higher resolution compared to FWI with the Marmousi2 data. A major benefit is that the extended source should provide much greater illumination of the subsurface compared to primary reflections, and an attendant improvement in imaging below salt.

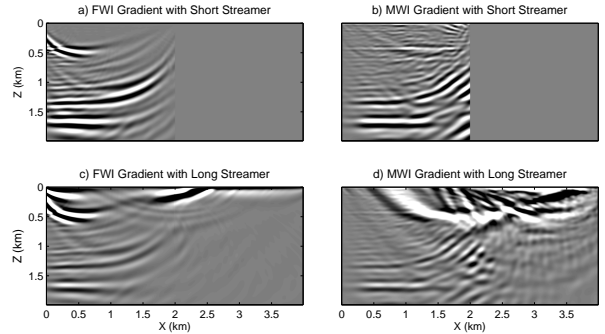


Figure 3: a) FWI and b) MWI misfit gradients for synthetic data computed for a streamer with a length of 2 km. c) FWI and d) MWI misfit gradients for synthetic data computed for a streamer with a length of 4 km.